Asymmetric Planetary Nebulae III
ASP Conference Series, Vol. 313, 2004
M. Meixner, J. Kastner, B. Balick and N. Soker eds.

Three-Dimensional Photoionization Modelling of the Hydrogen-Deficient Knots in the Planetary Nebula Abell 30

B. Ercolano, M. J. Barlow, P. J. Storey

University College London, Gower Street, London WC1E 6BT, UK

X.-W. Liu

Department of Astronomy, Peking University, Beijing, 100871, China

T. Rauch[1], K. Werner

Institut für Astronomie und Astrophysik, Abt. Astronomie, Sand 1, Universität Tübingen, 72076 Tübingen, Germany

Abstract. We have constructed a photoionization model, using the 3-D Monte Carlo code MOCASSIN for one of the hydrogen-deficient knots (J3) of the born-again planetary nebula Abell 30. The model consists of spherical knots, comprising a cold, dense, hydrogen-deficient core with very high metal abundances. The inner core, occupying 9.1% of the total volume of the knot, is surrounded by a less dense hydrogen-deficient and metal-enriched gas envelope, with less extreme abundances. The envelope of the knot might have been formed by the mixing of the knot material with the surrounding nebular gas.

The chemical abundances inferred from our modelling of the central core region and of the envelope of the knot are, at least qualitatively, in agreement with the abundances derived by the empirical analysis of Wesson et al. (2003), although the discrepancies between the core and the envelope abundances that we find are less dramatic than those implied by the ORL and CEL empirical analysis. Our models also indicate, in agreement with the empirical analysis of Wesson et al. (2003), that the C/O ratio in the two regions of the knot is less than unity, contrary to theoretical predictions for born-again nebulae (Herwig et al., 2001) .

1. Introduction

Recent empirical analysis based on new observational data of knot J3 of Abell 30 (Wesson et al. 2003) found large discrepancies between the ionic abundances measured from optical recombination lines (ORLs) and those measured from collisionally excited lines (CELs). Harrington & Feibelman (1984) proposed that

[1]Dr.-Remeis-Sternwarte, Sternwartstraße 7, D-96049 Bamberg, Germany

this discrepancy could be explained if very large temperature variations were present within the knots of Abell 30. A high concentration of heavy elements in the core of the knots could create a very cool (≈1000 K) but still ionized region emitting the observed ORLs. This could be surrounded by a hotter region consisting of material with more typical nebular abundances emitting the observed CELs. The analysis of Wesson et al. (2003) is in agreement with this interpretation.

2. Dust-heated Photoionization Modelling

The three-dimensional photoionization code, MOCASSIN, described by Ercolano et al. (2003a), was used in this work, since this code can self-consistently treat asymmetries and density and chemical inhomogeneities.

Table 1. Model elemental abundances in the two assumed regions (dense, cold core and thin hotter outer region) of the knot J3 in Abell 30. Also listed, in columns 3 and 5, respectively, are empirical elemental abundances from the whole knot, derived from ORLs and from CELs Wesson et al. (2003). The abundances are given by number with respect to helium.

	Core	ORLs	Env.	CELs
H/He	0.0250	0.0850	0.025	0.085*
C/He	0.0200	0.0389	$1.25{\cdot}10^{-3}$	$1.41{\cdot}10^{-4}$
N/He	0.0222	0.0229	$1.87{\cdot}10^{-3}$	$6.76{\cdot}10^{-5}$
O/He	0.0233	0.1071	$3.50{\cdot}10^{-3}$	$1.78{\cdot}10^{-4}$
Ne/He	0.0200	0.0831	$4.00{\cdot}10^{-3}$	$5.13{\cdot}10^{-4}$

* No estimate for the helium abundance was available to Wesson et al. (2003) from CELs. H/He was assumed to be equal to the value they obtained from the ORL analysis.

The failure of our preliminary gas-only models to produce temperatures high enough for the emission of the observed CELs indicates that photoionization of He and heavy elements alone cannot, in the virtual absence of hydrogen, provide enough heating to account for the collisionally excited emission lines observed. A good candidate for the additional energy source, needed to produce the extra heating, is photoelectric emission from dust grains. A radiative transfer treatment for dust grains has not yet been implemented in the radiative transfer of MOCASSIN, although work is already in progress in this direction. Nevertheless, in this work we estimated the heating provided by photoelectric emission from the grains by using a strategy similar to that already used by Borkowski & Harrington (1991) for the modelling of the grain-heated, dusty planetary nebula in M22. An outline of the method used in this work is given in Ercolano et al. (2003b).

The final model consisted of a spherical knot composed of two phases: a dense inner nucleus ($N_{\rm He}$(core) ≈ 10,500 cm^{-3}), with a radius equal to 0.45 of

Table 2. Adopted parameters for the final Abell 30 knot J3 photoionization model

$\log(L/L_\odot)$	3.70	R_{core}	$0.45 \cdot R_{knot}$
T_*	130,000 K	N_{He}(core)	10,400 cm^{-3}
log g	6.0	N_{He}(env)	1680 cm^{-3}
D_{knot}	$1.68 \cdot 10^{17}$cm	ρ_d/ρ_g(core/env)	0.077/0.107
R_{knot}	$4.50 \cdot 10^{15}$cm	a_d	$1.0 \cdot 10^{-6}$cm

D_{knot}: distance of the centre of the knot from the ionizing source
R_{knot}: radius of the hydrogen-deficient knot
R_{core}: the radius of the thick, cold inner core of the knot
N_{He}(core): helium density by number [cm^{-3}] in the inner core of the knot
N_{He}(env): helium density by number [cm^{-3}] in the outer region of the knot
ρ_d/ρ_g: dust-to-gas ratio by mass in the core and in the envelope of the knot
a_d: radius of the dust grains

the total radius of the knot, $R_{\rm knot}$ (where $R_{\rm knot} = 4.50 \cdot 10^{15}$cm), surrounded by a less dense outer region ($N_{\rm He}$(env) $\approx$ 1700 cm^{-3}), occupying the remaining volume of the knot. Although the central core region only occupies about 9.1% of the total volume of the knot, its higher density and higher metal abundance means that a significant fraction of the total mass of the knot (43.9%) resides in this volume. As for the preliminary modelling the starting abundances were taken to be the empirical values obtained from CELs and from ORLs for the envelope and the core regions of the knot, respectively. The abundances were then adjusted, together with the other model parameters, in an iterative fashion in order to fit the the observed emission line spectrum. The final elemental abundances adopted for the two regions are summarised in Table 1, together with the empirical abundances derived by Wesson et al. (2003). The abundances for the outer region and for the cold dense core, where most of the ORL emission is produced, are given by number with respect to helium (columns 4 and 2, respectively, in Table 1), since this is the most abundant element. The abundances in the core are compared to the empirical ORL abundances of Wesson et al. (2003), which are also given by number with respect to helium in column 3 of Table 1. Most of the CEL emission is believed to be produced in the hotter envelope of the knot and, therefore, the model abundances in this region (column 4 of Table 1) are compared with the empirical CEL abundances (column 5 of Table 1). It is clear from Table 1, however, that the final model abundances are quite different from the starting values which were taken to be equal to the values derived empirically. It should be noted at this point that, in Wesson et al.'s analysis, the abundances were derived without taking into account the possibility of chemical and density inhomogeneities within the knot, which would give rise to regions with different ionization structures. This implies a certain degree of freedom in the choice of abundances for our photoionization model. In light of this, the discrepancies existing between model and empirical abundance values are easily explained. We discuss in Section 4 the implications of our model abundances in the light of Wesson et al.'s empirical analysis.

Table 2 lists the parameters used for the final simulation.

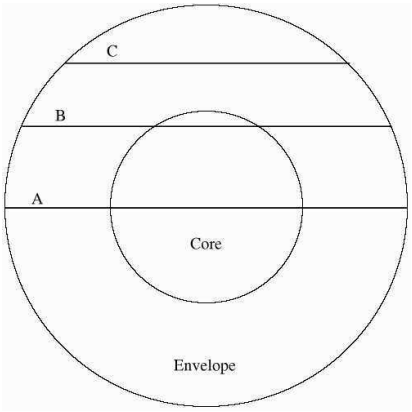

Figure 1. Schematical representation of a cross-section through the centre of the knot. The three rays, labelled A, B and C, correspond to the positions for which the model thermal contributions are plotted in Figure 2. The stellar field is assumed to be incoming from the left-hand side.

3. Abell 30 model results: The Thermal Balance

From the analysis of the heating and cooling contributions obtained at each location in our model grid, it appears that dust grains play the leading role in the heating of the knot in the envelope, dominating over the heating produced by photoionization of helium, which is the most abundant element, and by other elements (including the small quantity of hydrogen remaining in the knot). This is very clearly visible in cross-sections through the knot (Figure 1), i.e., in the left-hand panels of Figure 2, where the heating and cooling contributions due to all the energy channels considered in our simulation are plotted as a function of radius. These include cooling by collisionally excited emission lines, cooling by free-free and recombination continuum radiation and heating by photoionization and photoelectric emission from dust grains. The corresponding helium ionic fractions and the electron temperatures are plotted on the right-hand panels of Figure 2, also as a function of radius. The plots correspond to three cuts through the knot, namely cut A (top panels), cut B (middle panels) and cut C (bottom panels). These are labelled in Figure 1.

Heating from atomic photoionization is dominant in the inner regions of the knot since the abundance of singly ionized helium (or neutral helium, in the case of cut A) is highest there, due to the sixfold density increase in this region. The shadowing effect of the dense core is clearly visible in cut A, causing heating by photoionization to decrease sharply already within the inner region of the knot. Heating by photoelectron emission from dust grains is higher in the envelope of the knot, where the radiation field is stronger. In fact, $G_{\rm d}(\nu)$, the frequency dependent contribution to the heating due to dust grains, is proportional to the flux, $F(\nu)$ and to the dust-to-gas ratio. The drop of 30% in the value of

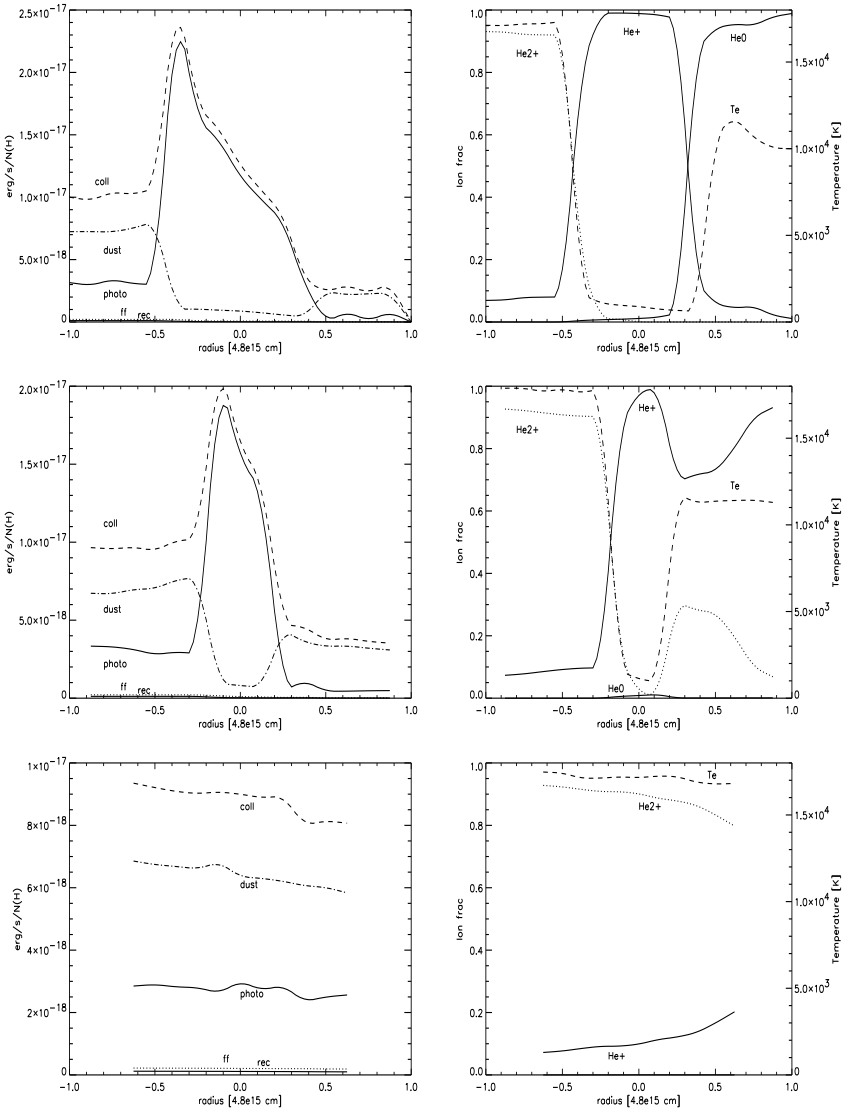

Figure 2. *Left panels:* Heating and cooling contributions for knot J3 of Abell, plotted as a function of radius for three different cuts (from top to bottom: cuts A, B and C as shown in Figure 1).(*photo*: photoelectric heating by atoms and ions; *dust* photoelectric heating by dust grains; *coll*: collisional cooling by ions; *ff*: cooling by free-free radiation; *rec*: cooling by recombination). *Right panels:* Corresponding fractional ionic abundances for helium and electron temperatures, plotted as a function of radius.

the dust-to-gas ratio from the envelope to the core is not sufficient to explain the drop in the grain heating shown in Figure 2, so this must be mainly due to the drop in $F(\nu)$, especially the attenuation of radiation at $h\nu > 54.4\,eV$. In the shadowed region, $F(\nu)$ is dominated by the softer diffuse component of the radiation field, the stellar photons having been mostly absorbed within the dense core. For this reason dust heating will make a smaller contribution in the shadowed region, as confirmed by Figure 2.

4. Conclusions

We have constructed a photoionization model for the hydrogen-deficient knot J3 of Abell 30. This consisted of a spherical blob with a very dense metal rich core, surrounded by a layer of less dense gas, with somewhat less enhanced metal abundances. The envelope region composition might be formed by the mixing of the outer layers of the knot with the surrounding nebular gas. Our models show that chemical and density homogeneities alone were not sufficient to create enough heating to explain the collisionally excited lines (CELs) observed in the spectrum of the knot (see, for instance, Wesson et al., 2003).

Following the hypothesis of Borkowski & Harrington (1991), heating by photoelectric emission from dust grains was introduced into the model. Although using a simplified approach, this work has shown that for a grain radius of $10^{-6}\,cm$ a dust-to-gas ratio, ρ_d/ρ_g, of 0.107 by mass is sufficient to provide enough heating to the envelope of the knot to fit the CEL spectrum. Although the final value used for our model is about 10 times larger than the value of 0.01-0.02, thought to be typical for the interstellar medium, this is not surprising, as the actual amount of dust mixed with the gas in these types of object is very uncertain. Borkowski & Harrington (1991) inferred even larger dust-to-gas mass ratios, between 0.17 and 0.62, from their study of the dusty H-deficient planetary nebula in M22. However, as discussed by Ercolano et al. (2003b), the dust-to-gas ratio in the equatorial knots of Abell 30 is expected to be higher than in the polar knots (Harrington, Borkowski & Tsvetanov 1997), hence higher than the value of 0.107 found here for the envelope of the polar knot J3.

Final abundances derived for the two regions of the knot show core/envelope abundance ratios ranging from 5 for neon to 16 for carbon; these are somewhat less dramatic than the ratios of 300-700 found from the ORL/CEL abundance analysis of Wesson et al. (2003), but nevertheless follow the same trend. It should also be noticed, when comparing our abundances with those derived by Wesson et al., that the empirical results they obtained were based on the assumption of a chemically/density homogeneous knot, with a constant ionization structure. However, this is not likely to be the case since it is clear from Fig. 2 that the ionization structure is very different in the inner and outer regions of the knot. In particular, the abundance of oxygen derived from empirical analysis is very susceptible to the empirical ionization correction used and would change considerably if a bi-phase empirical analysis were to be carried out. Nevertheless, in agreement with Wesson et al.'s empirical analysis, our models find both phases of the knot to be oxygen-rich, with C/O ratios of 0.86 and 0.36 in the core and the envelope of the knot, respectively. This is in contrast to theoretical predictions

for PNe in the born-again scenario which predicts C/O ratios larger than unity (Iben & Renzini, 1983; Herwig, 2001).

References

Borkowski, K., J., & Harrington, J., P., 1991, ApJ, 379, 168

Ercolano, B., Barlow, M. J., Storey, P. J., & Liu, X.-W., 2003a, MNRAS, 340, 1136

Ercolano, B., Barlow, M. J., Storey, P. J., Liu, X.-W., Rauch, & T., Werner, K., 2003b, MNRAS, 344, 1145

Harrington, J., P., & Feibelman, W., A., 1984, ApJ, 277, 716

Harrington, J. P., Borkowski, K., J., & Tsvetanov, Z., I., 1997, in Planetary Nebulae Vol. 180 ofIAU Symp. p. 235

Herwig, F., 2001, Ap&SS, 275, 15

Iben, I., J., & Renzini, A., ARA&A, 21, 271

Wesson, R., Liu, X.- W., & Barlow, M., J., 2003, MNRAS, 340, 253